DALTON
FULL PAPER

cis- and *trans*-nitrosyltetraammineruthenium(II). Spectral and electrochemical properties and reactivity

Maria G. Gomes,[a] **Celso U. Davanzo,**[b] **Sebastião C. Silva,**[c] **Luiz G. F. Lopes,**[c] **Paulo S. Santos**[d] **and Douglas W. Franco** *[,c]

[a] *Universidade Federal do Ceará, Departamento de Química Analítica e Físico-Química, Fortaleza, CE, Brasil*
[b] *Instituto de Química, Universidade Estadual de Campinas, Campinas, SP, Brasil*
[c] *Instituto de Química de São Carlos, USP, Caixa Postal 780, 13560-970, São Carlos-SP, Brasil*
[d] *Instituto de Química, USP, São Paulo, SP, Brasil*

A synthetic route was developed for the preparation of *trans*-$[Ru(NH_3)_4(NO)X]^{n+}$, where X = isonicotinamide (isn), pyrazine (pyz) or sulfite, and *cis*-$[Ru(NH_3)_4(NO)(NO_2)]^{2+}$. The complexes have been characterized by elemental analysis, UV/VIS, infrared, ^1H NMR and ESR spectroscopies, molar conductance measurements and cyclic voltammetry. All showed ν(NO) in the range characteristic of metal-co-ordinated NO^+ and do not exhibit any ESR signal, consistent with the formulation of $Ru^{II}–NO^+$. The equilibrium constants K_{eq} for the reaction *trans*-$[Ru(NH_3)_4(NO)X]^{3+} + 2OH^- \rightleftharpoons$ *trans*-$[Ru(NH_3)_4(NO_2)X]^+ + H_2O$ are 2.5×10^8 and 6×10^8 dm^6 mol^{-2} for X = isn or pyz. Cyclic voltammograms of the complexes in aqueous solution exhibited reversible one-electron waveforms in the potential range −0.13 to −0.38 V *vs.* SCE, which were assigned to the $[Ru(NH_3)_4(NO)X]^{n+} \longrightarrow [Ru(NH_3)_4(NO)X]^{(n-1)+}$ process. Nitric oxide and *trans*-$[Ru(NH_3)_4(H_2O)X]^{2+}$ are the final products of the reaction between Eu^{II} and *trans*-$[Ru(NH_3)_4(NO)X]^{3+}$, L = isn or pyz. *Ab initio* molecular orbital calculations performed for *trans*-$[Ru(NH_3)_4(NO)(pyz)]^{3+}$ and *trans*-$[Ru(NH_3)_4(NO)(pyz)]^{2+}$, and the products of the *trans*-$[Ru(NH_3)_4(NO)(pyz)]^{3+}$ one-electron electrochemical or chemical reduction, strongly suggest the added electron is localized mainly on the nitrosyl ligand. A correlation was observed between ν(NO) and $E_{\frac{1}{2}}$ for the reversible reduction wave. These results indicate that the nitric oxide reduction is facilitated by strong π-acceptor ligands *trans* to the NO. Nitric oxide and *trans*-$[Ru(NH_3)_4(H_2O)X]^{3+}$ were formed when solutions containing *trans*-$[Ru(NH_3)_4(NO)X]^{3+}$ were irradiated in the range 310–370 nm.

Advances in the chemistry of co-ordinated nitric oxide were mainly motivated by the important role that NO plays in air pollution.[1] Each year 10^6 tons (1 ton ≈ 1016 kg) of nitrogen oxides (NO and NO_2) are produced in fossil-fuel combustion processes, mainly as NO.

Despite its thermodynamic instability,[1] NO is kinetically inert with respect to decomposition and reduction, and requires the presence of metal or metal oxide[2] catalysts for many of its reactions. In these systems[1–5] the NO ligand reactivity is markedly influenced by the co-ordination-sphere characteristics of the metal center. Nitric oxide is also a versatile and important molecule in a wide variety of physiological processes,[3] including neurotransmission, immune regulation, smooth muscle relaxation, neuromodulation and platelet inhibition.[4] Therefore, it is not surprising that the use of metallonitrosyl complexes as agents potentially capable of releasing or removing NO *in vivo* has recently become a very active area of research.[5]

Aiming to learn more about the mutual influences of the ancillary ligands and NO upon their respective reactivities and using ruthenium ammines as a model, this paper describes the complexes *trans*-$[Ru(NH_3)_4(NO)X]^{n+}$ [X = isonicotinamide (isn), pyrazine (pyz) or SO_3^{2-}] and *cis*-$[Ru(NH_3)_4(NO)(NO_2)]Br_2$.

Experimental

Chemicals and reagents

Isonicotinamide and pyrazine (Aldrich) were used as supplied.

All preparations and measurements were carried out under an argon atmosphere, using standard techniques for manipulation of air-sensitive compounds.

Apparatus

All UV/VIS spectra were recorded on a Hewlett-Packard HP 8452A diode-array spectrophotometer. Owing to the fact that some bands are not well defined, a spectral curve fitting was carried out for the electronic spectra, assuming that the bands have a gaussian shape. Infrared spectra were recorded on a Bomem MB series FT-IR spectrometer. Analysis of ruthenium was performed in a Hitachi Z-8100 atomic absorption spectrophotometer, following the literature method.[6]

The ESR spectra were recorded on a Bruker ESP 300E spectrometer at liquid-nitrogen temperature, NMR spectra in D_2O on a Bruker AC-200 spectrometer. 3-(Trimethylsilyl)propanesulfonic acid was used as an internal standard.

A Digimed model CD-21 conductimeter was used for conductance measurements in water. A table of conductance for 13 nitrosyl complexes in water, all well described in the literature, was prepared. Our data indicate that 1 : 1 complexes exhibit conductances in water at 25 °C in the range 140–213, 1 : 2 complexes in the range 228–308 and 1 : 3 complexes in the range 431–570 ohm^{-1} cm^2 mol^{-1}. The conductometric data for the complexes are in good agreement with the formulations *trans*-$[Ru(NH_3)_4(NO)(isn)][BF_4]_3$, *trans*-$[Ru(NH_3)_4(NO)(pyz)][BF_4]_3$, *trans*-$[Ru(NH_3)_4(NO)(SO_3)]Cl$ and *cis*-$[Ru(NH_3)_4(NO)(NO_2)]Br_2$, which yield Λ_M 552, 502, 147 and 245 ohm^{-1} cm^2 mol^{-1}, respectively.

Electrochemical measurements were made using a Parc Polarographic model 264A Analyzer/Stripping Voltammeter and model 0089 XY Recorder. A Methron-type three-electrode cell was used. Vitreous carbon, platinum wire and SCE were used as working, auxiliary and reference electrodes, respectively. Purified Ar was used for deaeration of the cell. The electrochemical reversibility was checked[7] by use of the differences in anodic and cathodic peak potentials and the ratio I_{pa}/I_{pc} and plots of I_p *versus* $v^{\frac{1}{2}}$.

The photolysis experiments were performed according to the procedures described previously.[8] The irradiations were carried out by using an Osram 200 W Hg–Xe lamp in an Oriel model 6292 Universal arc-lamp source with an Oriel interference filter (≈10 nm band pass). Photolysis was done in aqueous trifluoracetic acid solutions containing 1.0×10^{-3} to 5×10^{-4} mol dm^{-3} of the ruthenium complex. Solutions for the photolysis and dark reactions were prepared in the same way. Corrections were made for thermal reactions during photolysis by using the dark unirradiated sample as a blank.

Since the voltammograms (cyclic voltammetry, CV; differential pulse polarography, DPP) and the electronic spectra of the photolysed and the dark solutions are quite different, both techniques could be used for quantum-yield measurements. However, for convenience, the spectrophotometric technique was chosen for quantum-yield determinations of *trans*-$[Ru(NH_3)_4(H_2O)(isn)]^{3+}$ ($\lambda = 314$ nm, $\varepsilon = 8.5 \times 10^4$ dm^3 mol^{-1} cm^{-1}) and *trans*-$[Ru(NH_3)_4(NO)(isn)]^{3+}$ ($\lambda = 323$ nm, $\varepsilon = 3.2 \times 10^2$ dm^3 mol^{-1} cm^{-1}). For quantum-yield determinations, samples subjected to irradiation were periodically monitored by recording the UV/VIS spectra. Quantum yields were calculated only for solutions where photolysis did not exceed 10%.

Preparation of ruthenium complexes

The complex *cis*-$[Ru(NH_3)_4(NO)(OH)][ClO_4]_2$ was prepared as described by Pell and Armor[9] and *trans*-$[Ru(NH_3)_4(SO_2)Cl]Cl$ by following the method of Isied and Taube.[10]

***trans*-$[Ru(NH_3)_4(SO_4)X]Cl$ (X = isn or pyz).** The compounds were prepared by adapting the literature procedures.[11] The complex *trans*-$[Ru(NH_3)_4(SO_2)Cl]Cl$ (0.200 g, 0.65 mmol) was dissolved in argon-degassed water (3 cm^3) and a ten-fold excess of isonicotinamide or pyrazine added. Following this, 6 mol dm^{-3} HCl (2 cm^3) and 30% H_2O_2 (5 cm^3) were immediately added to the reaction flask, resulting in a yellow solution. An excess (≈30 cm^3) of acetone was added and the solution allowed to stand in a freezer for 4 h. The solid was filtered off, washed with acetone, and dried under vacuum; yields varied from 62 (pyz) to 83% (isn) {Found: C, 12.87; H, 4.06; N, 22.18; Ru, 25.94. Calc. for *trans*-$[Ru(NH_3)_4(SO_4)(pyz)]Cl$: C, 12.60; H, 4.20; N, 22.06; Ru, 26.55. Found: C, 17.81; H, 4.37; N, 20.10; Ru, 23.40. Calc. for *trans*-$[Ru(NH_3)_4(SO_4)(isn)]Cl$: C, 17.03; H, 4.26; N, 19.87; Ru, 23.91%}.

***trans*-$[Ru(NH_3)_4(NO)X][BF_4]_3$ (X = isn or pyz).** The complex *trans*-$[Ru(NH_3)_4(SO_4)(isn)]Cl$ (0.100 g, 0.24 mmol) was dissolved in HBF_4 solution (5 cm^3) with the pH previously adjusted to 5.5. The complex was reduced with Zn(Hg) in a stream of argon for 30 min (10 min for the pyrazine derivative). The resulting solution was transferred to a vessel containing 4.9 mol dm^{-3} HBF_4 (1.5 cm^3) and $NaNO_2$ (0.100 g, 1.45 mmol). The solution first turned yellow, then pale pink. An excess of ethanol was added and the solution allowed to stand in a freezer for 2 h. The product was filtered off, washed with ethanol and dried under vacuum. Yields: 67 (isn) and 63% (pyz) {Found: C, 12.60; H, 3.41; N, 16.76; Ru, 17.37. Calc. for *trans*-$[Ru(NH_3)_4(NO)(isn)][BF_4]_3$: C, 12.38; H, 3.10; N, 16.84; Ru, 17.36. Found: C, 8.82; H, 3.12; N, 18.36; Ru, 19.09. Calc. for *trans*-$[Ru(NH_3)_4(NO)(pyz)][BF_4]_3$: C, 8.89; H, 2.97; N, 18.16; Ru, 18.73%}. Infrared data (cm^{-1}): L = isn, 3420–3350 [$\nu(NH_2)$ and $\nu(NH_3)$], 3248–3147 [$\nu(NH_3)$], 1923 [$\nu(NO)$], 1688 (amide I), 1628 [amide II and $\delta(NH_3)$], 1558–1425 [ν(ring)], 1385 (amide III), 1348–1202 [ν(ring)], 1107 [$\nu(BF_4)$], 854 [δ(C–H) out of plane], 750 [$\rho(NH_3)$], 619 [ν(Ru–NO)] and 484 [$\nu(Ru–NH_3)$]; L = pyz, 3304–3215 [$\nu(NH_3)$], 1942 [$\nu(NO)$], 1626 [$\delta(NH_3)$], 1429 [ν(ring)], 1366 [ν(ring) and $\nu_{sym}(NH_3)$], 1068 [ν(ring) and $\nu(BF_4^-)$], 874 [δ(C–H) out of plane], 827–739 [$\rho(NH_3)$], 621 [ν(Ru–NO)] and 476 [$\nu(Ru–NH_3)$].

***trans*-$[Ru(NH_3)_4(NO)(SO_3)]Cl$.** The complex *trans*-$[Ru(NH_3)_4(SO_2)Cl]Cl$ (0.100 g, 0.33 mmol) was dissolved in 0.1 mol dm^3 $NaHCO_3$ aqueous solution (4 cm^3) in a stream of argon for 15 min then transferred to a flask containing 6 mol dm^{-3} HCl (4 cm^3) and $NaNO_2$ (0.100 g, 1.45 mol). A pale yellow solid was precipitated upon the addition of ethanol (10 cm^3), which was filtered off and dried under vacuum. The solid was redissolved in water and transferred to a glass tube packed with octadecyl resin (C_{18}) and eluted with water. The liquid collected was then evaporated (40 °C) until a solid appeared; the solution was cooled, the compound isolated on a filter, washed with ethanol and dried under vacuum. Yield: 75% {Found: H, 3.75; Cl, 11.61; N, 22.28; Ru, 32.85; S, 10.21. Calc. for *trans*-$[Ru(NH_3)_4(NO)(SO_3)]Cl$: H, 3.81; Cl, 11.29; N, 22.25; Ru, 32.13; S, 10.17%}. Infrared data (cm^{-1}): 3261 [$\nu(NH_3)$], 1871 [$\nu(NO)$], 1628 [$\delta(NH_3)$], 1319 [$\delta_{sym}(NH_3)$], 1094 [$\nu_{deg}(SO_3)$], 997 [$\nu_{sym}(SO_3)$], 837–775 [$\rho(NH_3)$], 642 [$\delta(SO_3)$], 598 [ν(Ru–NO)] and 501 [$\nu(Ru–NH_3)$].

$[(NO)(NH_3)_4RuSSRu(NH_3)_4(NO)]Cl_6{\cdot}H_2O$. Zinc amalgam was added to a solution prepared by dissolving *trans*-$[Ru(NH_3)_4(NO)(SO_3)]Cl$ (0.300 g, 0.95 mmol) in 0.05 mol dm^{-3} HCl (100 cm^3). The yellow solution turned blue and after a few minutes green. After 10 min it was filtered in a glove-bag and transferred immediately to a column containing Bio-Rad Dowex 500W-X8 resin (200–400 mesh), previously washed with 0.25 mol dm^{-3} NaCl (300 cm^3) and 0.05 mol dm^{-3} HCl (100 cm^3). The green species was eluted with 4.0 mol dm^{-3} HCl. During the whole elution process the system was kept under an argon atmosphere. The resulting green solution was evaporated to dryness under vacuum at 40–50 °C. Yield: 15% (Found: H, 3.94; Cl, 30.39; N, 20.65; Ru, 29.63. Calc.: H, 3.75; Cl, 30.73; N, 20.79; Ru, 29.16%).

***cis*-$[Ru(NH_3)_4(NO)(NO_2)]Br_2$.** The complex *cis*-$[Ru(NH_3)_4(NO)(OH)][ClO_4]_2$ (0.33 g, 0.079 mmol) was dissolved in argon-degassed water (3 cm^3) and concentrated HBr (0.2 cm^3) added. The pink solution became yellow. After the addition of $NaNO_2$ (0.100 g, 1.45 mol) an orange-yellow solid precipitate was filtered off, washed with ethanol, and dried under vacuum. Yield: 74% {Found: Br, 39.60; H, 2.80; N, 20.77; Ru, 24.96. Calc. for *cis*-$[Ru(NH_3)_4(NO)(NO_2)]Br_2$: Br, 39.46; H. 2.96; N, 20.74; Ru, 24.96%}. Infrared data: 3228–3148 [$\nu(NH_3)$], 1927 [$\nu(NO)$], 1628–1533 [$\delta_{deg}(NH_3)$], 1425 [$\nu_{asym}(NO_2)$], 1310 [$\delta_{sym}(NO_2)$ and $\delta(NH_3)$], 972–835 [$\delta(NO_2)$ and $\rho(NH_3)$], 608 [ν(Ru–NO)] and 478 [$\nu(Ru–NH_3)$].

***trans*-$[Ru(NH_3)_4(NO_2)(isn)][BF_4]$.** The complex *trans*-$[Ru(NH_3)_4(NO)(isn)][BF_4]_3$ (0.100 g, 0.17 mmol) was dissolved in 1 mol dm^{-3} NaOH (3 cm^3). The brown-red solid was filtered off, washed with ethanol, and dried under vacuum. Yield: 92% {Found: C, 16.55; H, 4.27; N, 22.92; Ru, 23.82. Calc. for *trans*-$[Ru(NH_3)_4(NO_2)(isn)][BF_4]$: C, 16.98; H, 4.24; N, 23.12; Ru, 23.84%}.

Computational details

Ab initio calculations were carried out by using density functional theory (DFT). Gradient correction for exchange was made using Becke's three functional parameters[12] and the non-local correlation of Lee *et al.*[13] These corrections were included in the Becke 3LYP method, which is standard in the quantum-chemistry computational package GUASSIAN 94.[14] We have used the basis set 3-21g and or the double-zeta valence-polarized basis set DZVP-DFT.[15]

Table 1 Molecular orbital energy levels (cm^{-1}) of ions $[Ru(NH_3)_4(NO)(pyz)]^{n+}$

Orbital	$[Ru(NH_3)_4(NO)(pyz)]^{3+}$	$[Ru(NH_3)_4(NO)(pyz)]^{2+}$
π*(NO)		Unpaired (68 772)[a]
d_{z^2}	−111 160	−69 810 (−69 145)
$d_{x^2-y^2}$	−111 353	−70 045 (−69 834)
π*(NO)	−125 750	
π*(NO)(LUMO)	−125 930	
π*(pyrazine)		−72 404 (−72 847)
π*(NO)(LUMO)		−79 943 (−76 620)
π*(NO)(HOMO)		−99 900 (unpaired)
σ, π(pyrazine)		−114 430 (−114 313)
σ, π(pyrazine)(HOMO)	−139 946	
π_{py} (pyrazine)	−153 294	−120 505 (−120 338)
π_{py} (pyrazine)	−161 670	−134 451 (−134 125)
d_{yx}	−159 778	−115 547 (−115 369)
d_{yz}	−166 581	−118 683 (−118 628)
d_{xz}	−167 483	−121 005 (−115 854)

[a] Values in parentheses are for β orbitals.

Table 2 The UV/VIS spectral data for the ruthenium complexes

Complex	λ_{max}/nm	ε/$dm^3\ mol^{-1}\ cm^{-1}$	Assignment
trans-$[Ru(NH_3)_4(NO)(isn)][BF_4]_3$[a]	230[b]	1.4×10^4	MLCT
	268	1.3×10^3	d ⟶ d, π ⟶ π*(L)
	323	3.2×10^2	d ⟶ d
	486	4.4×10^1	d ⟶ π*(NO), L ⟶ π*(NO)
trans-$[Ru(NH_3)_4(NO)(pyz)][BF_4]_3$[a]	230[b]	1.0×10^3	MLCT
	276	4.4×10^3	d ⟶ d, π ⟶ π*(L)
	302	6.6×10^2	d ⟶ d
	468	4.0×10^1	d ⟶ π*(NO)
	584	4.3×10^1	L ⟶ π*(NO)
trans-$[Ru(NH_3)_4(NO)(SO_3)]Cl$[a]	224[b]	9.3×10^3	MLCT
	327	5.8×10^2	d ⟶ d
	364	3.5×10^2	d ⟶ d
	422	3.5×10^1	d ⟶ π*(NO)
cis-$[Ru(NH_3)_4(NO)(NO_2)]Br_2$[a]	249	1.8×10^3	MLCT
	285	3.0×10^2	d ⟶ d
	454	1.8×10^1	d ⟶ π*(N)

[a] Spectra were taken in 0.1 mol dm^{-3} CF_3CO_2H. [b] Doubtful value because of strong absorbance of the solvent (it absorbs until 230 nm).

Molecular orbital analyses for the $[Ru(NH_3)_4(NO)(pyz)]^{3+}$ complex and the reduced species $[Ru(NH_3)_4(NO)(pyz)]^{2+}$ were performed at the optimized geometry.

Results and Discussion

Molecular orbital analysis

The *ab initio* DFT geometry optimizations were performed in internally redundant coordinates, in a real C_1 symmetry. As input data we used an optimized geometry obtained at the semi-empirical level, using the Zindo1 method from the HYPERCHEM 4.5 package.[16]

Table 1 shows the calculated energy levels for the species $[Ru(NH_3)_4(NO)(pyz)]^{3+}$ and $[Ru(NH_3)_4(NO)(pyz)]^{2+}$. A very useful model for the metal nitrosyl complex treats the system as a six-co-ordinated MNO triatomic group, in C_{4v} symmetry.[17] However the molecular orbital structure of the $[Ru(NH_3)_4(NO)(pyz)]^{3+}$ ion shows some difference from this model, due to the presence of the internal pyrazine orbitals.

In the $[Ru(NH_3)_4(NO)(pyz)]^{3+}$ ion the LUMO is the degenerate π* orbital centered on the NO, which mixes with the metal d_π orbitals. Above the nitrosyl π-antibonding orbitals are the $d^*_{z^2}$ and $d^*_{x^2-y^2}$ antibonding orbitals of the ruthenium. The HOMO and the two orbitals below are located mainly on the pyrazine ligand. The HOMO corresponds to the lone-pair electron of the terminal nitrogen of the pyrazine, and is higher in energy (about 20 000 cm^{-1}) than the d_{xy} orbital. Of the d orbitals centered on ruthenium, the d_{xy} lies in the equatorial plane and does not interact with the NO or the axial ligand. The d_{yz} and the d_{xz} orbitals mix with the π-antibonding orbitals of the NO fragment and populate these antibonding orbitals in the ground state. Also due to the π interaction, the d_{yz} and d_{xz} orbitals are stabilized (about 7000 cm^{-1}) relative to the d_{xy} orbital.

The molecular orbital calculations for the reduced species $[Ru(NH_3)_4(NO)(pyz)]^{2+}$ localize the additional electron mainly in the NO-π* orbital which becomes the HOMO, about 15 000 cm^{-1} higher than the second occupied molecular orbital, that of the lone pair on the pyrazine. Also the calculated spin density is 94% localized on the NO fragment. So, according to the *ab initio* DFT calculations, we can say that in the $[Ru(NH_3)_4(NO)(pyz)]^{3+}$ species the NO behaves essentially as NO^0. This observation is consistent with measurements on the one-electron reduction of $[Ru(NH_3)_5(NO)]^{3+}$,[18a] $[RuCl(bipy)_2(NO)]^{3+}$,[18b,c] *trans*-$[Ru(Hdmg)_2Cl(NO)]$[18e] (Hdmg = dimethylglyoximate ion) and *trans*-$[Ru(NH_3)_4(NO)\{P(OEt)_3\}]^{3+}$.[19]

Electronic spectra

The UV/VIS spectral characteristics and band assignments for the new nitrosyl complexes are given in Table 2.

The complex *trans*-$[Ru(NH_3)_4(NO)(pyz)]^{3+}$ shows an intense band at 230 nm, assigned to a metal to pyrazine charge transfer. A band at 302 nm is assigned to the d–d spin-allowed transition and one at 276 nm to a second d–d spin allowed transition, considering that the occupied d orbitals are split by about 7000 cm^{-1} due to the interaction with the π* orbitals of

NO. However in this region an internal $\pi \longrightarrow \pi^*$ transition of pyrazine also occurs and these two bands ($d \longrightarrow d$ and $\pi \longrightarrow \pi^*$) are probably superimposed, making assignments very difficult. In addition, two other bands can be observed at 468 and 584 nm. The former is assigned to the $d_{xy} \longrightarrow \pi^*$(NO) transition. The lower-energy band is only observed when the axial ligand is an heterocyclic ring. According to the calculated molecular orbital levels, we tentatively assign this band to an interligand π(pyrazine) $\longrightarrow \pi^*$(NO) transition.[20] These assignments, except for the ligand-to-ligand charge-transfer band, are essentially the same as those made by Manoharan and Gray[21] for the $[Ru(CN)_5(NO)]^{2-}$ ion and suggest some changes in Schreiner's assignment for the $[Ru(NH_3)_4(NO)X]^{q+}$ type compounds.[22]

The *trans*-$[Ru(NH_3)_4(NO)(isn)]^{3+}$ ion exhibits an intense band at 230 nm assigned to the $Ru^{II} \rightarrow isn$ charge-transfer transition. The second band of medium intensity at 323 nm was assigned to a spin-allowed d–d transition. According to the molecular orbital calculation for *trans*-$[Ru(NH_3)_4(NO)(pyz)]^{3+}$, the lower-energy band at 486 nm could be assigned to a superposition of the interligand π(isn) $\longrightarrow \pi^*$(NO) transition and the metal to NO charge transfer, $d \longrightarrow \pi^*$(NO). Another intense band at 268 nm was tentatively assigned to a second d–d transition, superimposed on the isonicotinamide $\pi \longrightarrow \pi^*$ internal transition (free isonicotinamide shows this band at 268 nm in aqueous solution).

For *trans*-$[Ru(NH_3)_4(NO)(SO_3)]^+$ the band at 224 nm is assigned to the metal to ligand charge-transfer transition and those at 327 and 364 nm could be assigned to a spin-allowed d–d transition. The band of low intensity at 422 nm is assigned to a $d \longrightarrow \pi^*$(NO) charge-transfer transition.

The complex *cis*-$[Ru(NH_3)_4(NO)(NO_2)]^{2+}$ shows three bands in the UV/VIS spectrum. The band at 249 nm is assigned to a metal to ligand charge transfer, a band of medium intensity at 285 nm is assigned to a spin-allowed d–d transition and another band of low intensity at 454 nm is assigned to $d \longrightarrow \pi^*$(NO) charge-transfer transition.

Infrared spectra

The assignments made for the compounds described here are based on data for similar systems[9,23] (see Experimental section). The infrared spectra show N–O stretching frequencies in the 1871–1942 cm^{-1} region, and Ru–NO bands in the 598–739 cm^{-1} region.

The spectrum of *trans*-$[Ru(NH_3)_4(NO)(SO_3)]Cl$ shows bands at 1094, 997 and 642 cm^{-1} assigned to the SO_3 degenerate (deg) stretching, the symmetric stretching and the bending frequencies, respectively. This assignment follows Nakamoto[23] who suggested that the S-bonded sulfite group shows only two SO stretches between 1120 and 930 cm^{-1}.

For the *cis*-$[Ru(NH_3)_4(NO)(NO_2)]Br_2$ complex the symmetric stretching mode of NO_2 overlaps with the ammine band at 1310 cm^{-1}, however the asymmetric mode of NO_2 shows one sharp band at 1425 cm^{-1} and the bending frequency was observed at 835 cm^{-1}.

According to DFT molecular orbital calculations,[24] ν(NO) is somewhat dependent on the nature of the *trans* ligand, L. The ligand X, the ruthenium center and the ligand NO will interact along the z axis and the $4d_\pi$ orbital can be regarded as a bridge between X and NO. The weaker the π acidity of the ligand L, the more $4d_\pi$ electron density is transferred to the π^*(NO) orbital. Consequently, the NO stretching frequency decreases as the π-acceptor ability of L decreases.

^{1}H NMR spectra

The features of the ^{1}H NMR spectra for all complexes are consistent with the co-ordination of N-heterocyclic ligands. A proton chemical shift chart for the isn and pyz protons in the nitrosyl complexes is given in Fig. 1.

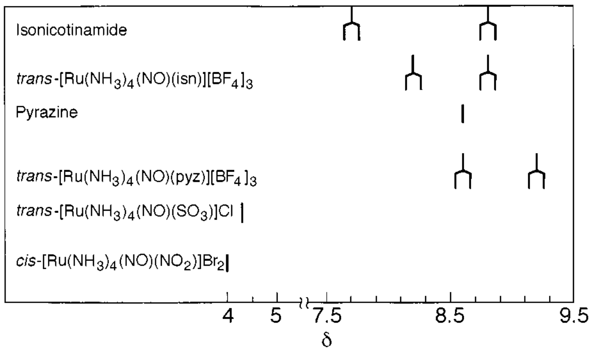

Fig. 1 Proton chemical shift chart for the N-heterocyclic protons in the nitrosyl complexes

The spectrum of free isn exhibits absorptions at δ 7.73 and 8.67, assigned to the *ortho*- and *meta*-protons. The pyz, as expected, shows only one signal at δ 8.63.

The ^{1}H NMR spectrum of *trans*-$[Ru(NH_3)_4(NO)(isn)][BF_4]_3$ shows one absorption at δ 8.22 attributed to the *o*-protons and another at δ 8.70 due to the *m*-protons. The complex *trans*-$[Ru(NH_3)_4(NO)(pyz)][BF_4]_3$ shows two absorptions at δ 8.65 (*meta*) and 9.22 (*ortho*).

The above complexes do not show a peak for the N–H protons of the ammines in D_2O. The absence of a broad peak for these protons (even in very concentrated solutions) suggests a rapid exchange of the ammine protons. Palmer and Basolo[25] noted that in a series of isoelectronic ammine complexes an increase in charge resulted in a marked increase in the rate of hydrogen exchange. Thus, the higher positive charge of the nitrosyl complex may be responsible in part for the enhanced rate of exchange of the ammine protons on *trans*-$[Ru(NH_3)_4(NO)(isn)]^{3+}$ and *trans*-$[Ru(NH_3)_4(NO)(pyz)]^{3+}$.

The ^{1}H NMR spectra of *trans*-$[Ru(NH_3)_4(NO)(SO_3)]^+$ and *cis*-$[Ru(NH_3)_4(NO)(NO_2)]^{2+}$ complexes show a broad peak for the N–H protons of the ammines in D_2O at δ 4.3 and 4.0, respectively. This is consistent with the charge effect,[26] since these species have overall charges of +1 and +2, which are lower than that of +3 for the above two complexes.

All the new nitrosyl complexes described in this work do not exhibit any signals in the ESR spectra. This fact is consistent with the formulation of NO^+ in the Ru–NO fragment.

Sulfite reactivity

In the complexes *trans*-$[Ru(NH_3)_4(SO_3)(H_2O)]$ and $[Co(NH_3)_5(SO_3)]^+$ the sulfite ligand is easily oxidized to sulfate[10,11] by action of air or H_2O_2. Therefore the resistance of the sulfite ligand in *trans*-$[Ru(NH_3)_4(NO)(SO_3)]^+$ to undergo oxidation to sulfate species is remarkable. Titration of *trans*-$[Ru(NH_3)_4(NO)(SO_3)]^+$ in acidic media ($c_{H+} \approx 10^{-1}$–1 mol dm^{-3}), with H_2O_2, $Ce(SO_4)_2$ and $KMnO_4$ leads to the consumption of less than 1 equivalent of oxidant per mol of complex. However *trans*-$[Ru(NH_3)_4(NO)(SO_3)]^+$ is quite reactive towards reducing agents. Upon treatment with Zn(Hg) and Cd(Hg), reduction of the sulfite ligand leads to the formation of a binuclear ruthenium tetraammine species which is bridged by a disulfide group, $[(NO)(NH_3)_4RuSSRu(NH_3)_4(NO)]Cl_6 \cdot H_2O$. Evolution of H_2S takes place upon a larger contact between the solution and the amalgam. The formation of the binuclear species was demonstrated by elemental analysis and by comparison of the electronic and vibrational spectra of the solid isolated with those described[26] for similar compounds. As observed for the $[\{Ru(NH_3)_5S\}_2]^{4+}$ ion, the electronic spectrum of $[\{(NO)(NH_3)_4RuS\}_2]^{6+}$ exhibits absorptions at 236 ($\varepsilon = 7.0 \times 10^3$), 332 ($3.1 \times 10^2$), 398 ($1.6 \times 10^2$) and 712 nm ($7.0 \times 10^2$ dm^3 mol^{-1} cm^{-1}). The last has been assigned in earlier studies of analogous compounds[26–29] to the chromophore RuSSRu.

The infrared spectrum of the binuclear complex reveals NO stretching frequencies of 1911 and 1847 cm^{-1}. In the Raman spectrum the S–S stretching was observed at 492 cm^{-1} in good agreement with what is expected from reported values for similar compounds.[26–29]

NO Reactivity

The chemical reactivity of co-ordinated NO depends on the mode of bonding.[1,2] Thus, linearly co-ordinated nitrosyls with ν(NO) higher than 1850 cm^{-1} are expected to undergo nucleophilic attack at the nitrosyl N atom.[2,30,31] We investigated the reactions of the present complexes with the nucleophilic agents OH$^-$, N$_3{}^-$, N$_2$H$_4$ and ON(CH$_3$)$_3$.

As far as the electronic spectra indicate, the nitrosyl complexes, at the concentration of 1.0×10^{-3} mol dm^{-3}, do not react with a ten-fold excess of N$_3{}^-$, N$_2$H$_4$ and ON(CH$_3$)$_3$ (range pH 1–8.5), 20 min after mixing. Nevertheless all react promptly with hydroxide ion giving deep yellow solutions. In the case of the *trans*-[Ru(NH$_3$)$_4$(NO)(isn)]$^{3+}$ the yellow color is due to the formation of a *trans*-[Ru(NH$_3$)$_4$(NO$_2$)(isn)]$^+$ species, which was isolated and characterized (see Experimental section), equation (1). Reconversion into the nitrosyl complex occurs by

$$\textit{trans}\text{-}[\mathrm{Ru(NH_3)_4(NO)(isn)}]^{3+} + 2\mathrm{OH}^- \rightleftharpoons \textit{trans}\text{-}[\mathrm{Ru(NH_3)_4(NO_2)(isn)}]^+ + \mathrm{H_2O} \quad (1)$$

acidification of the alkaline solution. The equilibrium constant for reaction (1) was measured by a spectrophotometric method[32] at 25.0 °C ± 0.1, as $K_{eq} = 2.5 \times 10^8$ dm^6 mol^{-2}. For the corresponding *trans*-[Ru(NH$_3$)$_4$(NO)(pyz)]$^{3+}$ system, using the same methodology, K_{eq} was estimated as 6×10^8 dm^6 mol^{-2}. For the same equilibrium, the following K_{eq} values have been reported: 1.6×10^9 for *cis*-[Ru(bipy)$_2$(NO)Cl]$^{2+}$,[33] 2.2×10^5 for *trans*-[Ru(NH$_3$)$_4$(NO)(py)]$^{3+}$, 5.9×10^7 for *trans*-[Ru(NH$_3$)$_4$(NO)(nic)]$^{3+}$ (nic = nicotinamide), 9.7×10^{10} for *trans*-[Ru(NH$_3$)$_4$(NO)(Him)]$^{3+}$ and 4.6×10^{13} dm^6 mol^{-2} for *trans*-[Ru(NH$_3$)$_4$(NO)(L-His)]$^{3+}$.[34]

The K_{eq} data are indicative of the completeness of the nitric oxide reaction and accordingly are expected to reflect, to some extent, the degree of nitrosonium character exhibited by the co-ordinated NO. Therefore, as suggested,[2] these equilibrium constant data should provide a straightforward way to compare the relative electrophilicity of the NO ligand. According to this proposition, the higher the electron deficiency in the NO fragment, as a consequence of the co-ordination sphere π acidity (mainly caused by the ligand *trans* to NO), the higher would be the driving force for the reaction of NO with OH$^-$.

For the *trans*-[Ru(NH$_3$)$_4$(NO)X]$^{3+}$ complexes above, calculated K_{eq} values decrease as L-His > Him > pyz >isn > nic > py, which except for the relative position of pyz and py follows the same trend[34] of increasing π-acceptor ability of X: L-His ≈ Him < py < isn < nic < pyz. This observation is not consistent with the reasoning above which would predict the complexes with the stronger π acceptors to have the higher values of K_{eq}. Probably the thermodynamic stability of the nitro species, which is included in K_{eq}, represents an important term in the driving force of this reaction and should be considered. Unfortunately the equilibrium constant data for the *trans*-[Ru(NH$_3$)$_4$(NO$_2$)X]$^{2+}$ species are not available, but are currently under investigation in our laboratory.

For *trans*-[Ru(NH$_3$)$_4$(NO)(SO$_3$)]$^+$, *trans*-[Ru(NH$_3$)$_4$(NO$_2$)(pyz)][BF$_4$] and *cis*-[Ru(NH$_3$)$_4$(NO)(NO$_2$)]$^{2+}$ a nitrite ⟶ nitrosyl interconversion occurs, but is not quantitative and loses reversibility above pH ≈ 11. Efforts to isolate the corresponding *trans*-[Ru(NH$_3$)$_4$(NO$_2$)(pyz)][BF$_4$] and the sodium salt of *trans*-[Ru(NH$_3$)$_4$(NO$_2$)(SO$_3$)]$^-$ have been unsuccessful.

Table 3 Electrochemical data for the ruthenium nitrosyl complexes and ν(NO) frequencies

Complex	$E_{\frac{1}{2}}$*/V	$\tilde{\nu}$(NO)/cm^{-1}	Ref.
[Ru(NH$_3$)$_5$(NO)]$^{3+}$	−0.40	1913	18(*a*)
trans-[Ru(NH$_3$)$_4$(NO)(SO$_3$)]$^+$	−0.38	1871	
trans-[Ru(NH$_3$)$_4$(NO)(Him)]$^{3+}$	−0.36	1923	34
trans-[Ru(NH$_3$)$_4$(NO)(L-His)]$^{3+}$	−0.35	1921	34
cis-[Ru(NH$_3$)$_4$(NO)(NO$_2$)]$^{2+}$	−0.26	1927	
trans-[Ru(NH$_3$)$_4$(NO)(py)]$^{3+}$	−0.23	1931	34
trans-[Ru(NH$_3$)$_4$(NO)(isn)]$^{3+}$	−0.19	1923	
trans-[Ru(NH$_3$)$_4$(NO)(nic)]$^{3+}$	−0.17	1941	34
trans-[Ru(NH$_3$)$_4$(NO){P(OEt)$_3$}]$^{3+}$	−0.14	1909	19
trans-[Ru(NH$_3$)$_4$(NO)(pyz)]$^{3+}$	−0.13	1942	
trans-[Ru(NH$_3$)$_4$(NO)(pic)]$^{4+}$	−0.24	1933	

* Potential *versus* SCE, $I = 0.20$ mol dm^{-3} Na(O$_2$CCF$_3$)–CF$_3$CO$_2$H, $c_{\mathrm{H}^+} = 10^{-4}$–$10^{-5}$ mol dm^{-3}, 25 °C.

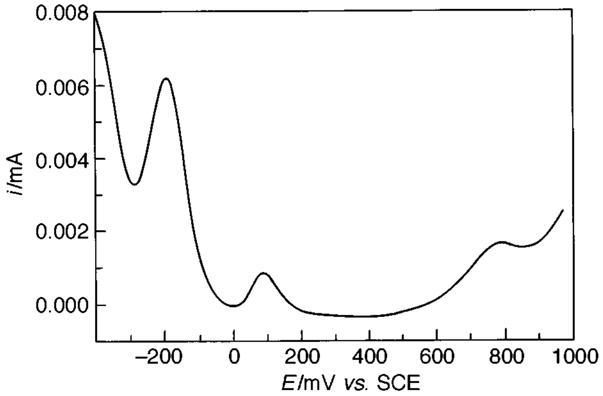

Fig. 2 Differential pulse polarogram for a solution of *trans*-[Ru(NH$_3$)$_4$(NO)(isn)][BF$_4$]$_3$. $I = 0.20$ mol dm^{-3} KCl, pH 4.60, 25 °C. $c_{\mathrm{Ru}} = 1.0 \times 10^{-3}$ mol dm^{-3}, pulse height 25 mV, 3 mV s^{-1}, $E_i = -0.400$ V

Cyclic voltammetry experiments showed that all the nitrosyl complexes exhibit a reversible one-electron process between −0.13 and −0.38 V *vs.* SCE (see Table 3). Since reversible electrochemical reductions of the NO ligand have been reported[1d,18,19] for complexes containing a linear MNO group in the same region of the voltammetric spectrum, this redox process was assigned to the reduction NO$^+$ + e $\rightleftharpoons$ NO at the co-ordinated NO$^+$. This assignment is supported by molecular orbital calculations (see Table 1) which localize the HOMO in the reduced species *trans*-[Ru(NH$_3$)$_4$(NO)(pyz)]$^{2+}$ on the π*(NO) orbital. Since no other electrochemical process was observed up to +1.2 V *vs.* SCE in the voltammetric scans of solutions containing the complexes described, we concluded that the ruthenium center is oxidized only at potentials higher than +1.2 V.

The NO$^+$ ⟶ NO^0 process in the species *cis*-[Ru(NH$_3$)$_4$(NO)(NO$_2$)]$^{2+}$, *trans*-[Ru(NH$_3$)$_4$(NO)(isn)]$^{3+}$ and *trans*-[Ru(NH$_3$)$_4$(NO)(SO$_3$)]$^+$ is reversible on the time-scale of the experiments (scan rates of 10 mV s^{-1}–1 V s^{-1}) suggesting that *trans*-[Ru(NH$_3$)$_4$(NO)(SO$_3$)], *trans*-[Ru(NH$_3$)$_4$(NO)(isn)]$^{2+}$ and *cis*-[Ru(NH$_3$)$_4$(NO)(NO$_2$)]$^+$ are reasonably stable.

For the complex *trans*-[Ru(NH$_3$)$_4$(NO)(pyz)]$^{3+}$, the process at $E_{\frac{1}{2}} = -0.13$ V is electrochemically reversible at scan rates >0.1 V s^{-1} and at temperatures <5 °C. At slower scan rates (⩽20 mV s^{-1}) or at room temperature the reduced species *trans*-[Ru(NH$_3$)$_4$(NO)(pyz)]$^{2+}$ does not live long enough to be reoxidized at the electrode.

The complex *trans*-[Ru(NH$_3$)$_4$(NO)(pyz)]$^{3+}$ is chemically reduced by europium(II) ions. This reaction consumes 1 mol of Eu$^{\mathrm{II}}$ per mol of nitrosyl complex. After this reaction the electrochemical process with $E_{\frac{1}{2}} \approx -0.13$ V is absent in the solution voltammogram whereas a new one is observed at $E_{\frac{1}{2}} \approx 0.17$ V which has been identified as due to the couple Ru$^{\mathrm{III}}$–Ru$^{\mathrm{II}}$ in *trans*-[Ru(NH$_3$)$_4$(H$_2$O)(pyz)]$^{2+}$. Also an electrochemical anodic wave, at $E_{pa} \approx 0.76 \pm 0.02$ V, can be observed. This last electrochemical process is probably due to oxidation of free NO.[35] The

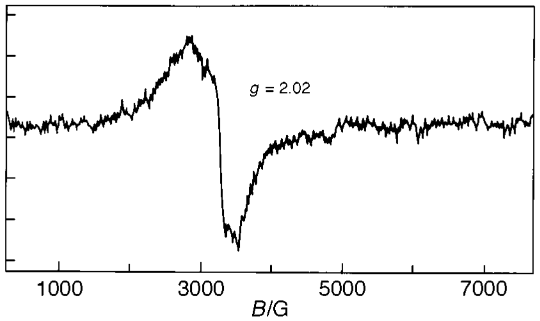

Fig. 3 The ESR spectrum of a frozen photolysed solution of *trans*-$[Ru(NH_3)_4(NO)(isn)][BF_4]_3$. Microwave power 100 mV, 77 K. Photolysis time 60 min; $\lambda_{irr} = 330$ nm, pH 3.60; $c_{Ru} = 1.0 \times 10^{-3}$ mol dm^{-3}

reaction of the nitrosyl species with Eu^{II} was also monitored by UV/VIS spectroscopy. After the addition of Eu^{II} to the solution containing *trans*-$[Ru(NH_3)_4(NO)(pyz)]^{3+}$ the band at $\lambda_{max} = 276$ nm ($\varepsilon = 4.4 \times 10^3$ dm^3 mol^{-1} cm^{-1}) disappeared and a new band at λ_{max} 474 nm ($\varepsilon = 1.5 \times 10^4$ dm^3 mol^{-1} cm^{-1}) appeared. The characteristics of the new band are consistent with the formation of *trans*-$[Ru(NH_3)_4(H_2O)(pyz)]^{2+}$. Ions *trans*-$[Ru(NH_3)_4(NO)(isn)]^{3+}$ when reduced at the electrode (see Fig. 2) or by Eu^{II} exhibit the same behavior as described above for *trans*-$[Ru(NH_3)_4(NO)(pyz)]^{3+}$ equation (2). Therefore, as far

$$trans\text{-}[Ru(NH_3)_4(NO)X]^{3+} + Eu^{II} + H_2O \longrightarrow trans\text{-}[Ru(NH_3)_4(H_2O)X]^{2+} + Eu^{III} + NO \quad (2)$$

as the electronic spectra and voltammograms (see Fig. 2) are concerned, the ions *trans*-$[Ru(NH_3)_4(NO)X]^{3+}$ (X = pyz or isn), after a one-electron reduction, exhibited a nitric oxide dissociation with formation of the aqua species.

Table 3 gives ν(NO) values for each of the nitrosyl complexes reported along with those of similar complexes and their potentials. There is, as expected, a direct relationship between the two parameters since both are dependent upon the electronic properties of the nitrosyl group. The most easily reducible NO^+ group is that bonded to the $[Ru(NH_3)_4(pyz)]^{2+}$ fragment, and the most resistant are the $[Ru(NH_3)_5]^{2+}$, $[Ru(NH_3)_4(SO_3)]$ and $[Ru(NH_3)_4(Him)]^{2+}$ moieties. This is not surprising since the pyz ligand is the strongest π acceptor in the series of ligands *trans* to NO^+ in the compounds listed in Table 3. The NH_3, SO_3^{2-} and Him ligands are better σ bases than pyz and do not compete with NO^+ for the ruthenium(II) $4d_\pi$ electrons. Instead they make more favorable the $Ru^{II} \rightarrow NO^+$ back bonding, through the $L{:}\rightarrow Ru^{II}$ σ interaction.

Photolysis experiments

The photochemical behavior of these complexes is now being investigated.[36] Solutions containing *trans*-$[Ru(NH_3)_4(NO)(isn)]^{3+}$ upon irradiation with light of 310–370 nm undergo the photochemical reaction (3). The voltammogram of the

$$trans\text{-}[Ru(NH_3)_4(NO)(isn)]^{3+} + H_2O \xrightarrow{h\nu} trans\text{-}[Ru(NH_3)_4(isn)(H_2O)]^{3+} + NO \quad (3)$$

photolysed solutions suggests the presence of *trans*-$[Ru(NH_3)_4(isn)(H_2O)]^{3+}$ ($E_{\frac{1}{2}}$ +0.10 V) and of free NO ($E_{pa} \approx +0.78$ V).[35] The presence of *trans*-$[Ru(NH_3)_4(isn)(H_2O)]^{3+}$ ions has also been confirmed through ESR spectroscopy ($g = 2.02$), see Fig. 3.

The quantum yield for the above reaction is 0.073 at 330 nm and exhibits no dependence in the pH (in the range 3.0–6.4) and on the presence of oxygen. However, for the same experimental conditions (pH, *I*, temperature) the quantum-yield data exhibit a wavelength dependence: 310 nm, $\varphi_{NO} = 0.040$; 370 nm, $\varphi_{NO} = 0.009$. No experimentally detectable NH_3 ligand photoaquation has been observed over the range of wavelengths investigated (310–370 nm).

Preliminary photolysis experiments[36] with *trans*-$[Ru(NH_3)_4(NO)X]^{3+}$, X = pyridine, 2-methylpyridine, pyrazine or nicotinamide, also indicate the formation of NO and *trans*-$[Ru(NH_3)_4(H_2O)X]^{3+}$ as a product.

In all these experiments the irradiations were performed using the ligand-field band (310–370 nm). Therefore, the population of an ^3E state is expected to increase. Since the observed reaction is of the photooxidation type it is likely that the population of the photoactive state is a product of the ^3E decay. This is consistent with what is expected[24] for ruthenium(II) nitrosyls in which the LUMO is localized on the π*(NO) orbital, the occupation of which by an electron will lead to the loss of NO. However, the quantum yields are wavelength dependent, suggesting the existence of more than one photoactive state.

Studies of the photochemical behavior of the mononuclear nitrosyl complexes, and of the electron-transfer processes in the binuclear $[\{(NO)(NH_3)_4RuS\}_2]^{6+}$, species are in progress at our laboratory.

The complexes *trans*-$[Ru(NH_3)_4(NO)(pyz)]^{3+}$ and *trans*-$[Ru(NH_3)_4(NO)(isn)]^{3+}$ are inert with respect to substitution reactions over a wide range of pH (1–8) on the time-scale of days. However dissociation of NO can easily be achieved by treating these complexes with reducing agents or by photolysis. Since the reduction potential for the $NO^+ + e \longrightarrow NO$ conversion in the above complexes is in the range of those of the biological reductors,[37] and these compounds show very low toxicity when tested on chinese hamster lung fibroblasts,[38] they may hold some promise as models for delivering intact NO in living systems.

Acknowledgements

The authors are very grateful to the Brazilian research foundations Fundação de Amparo à Pesquisa do Estado de São Paulo (FAPEP) (grant nos. 92/3515-3 and 95/0278-9), Fundação Coordenação de Aperfeiçoamento de Pessoal de Nível Superior (CAPES) and Conselho Nacional de Desenvolvimento Científico e Tecnológico (CNPq) for financial support and to Professor H. Taube and P. C. Ford for helpful discussions and encouragement. We also are very thankful to Professor Bruce R. McGarvey for reading the manuscript.

References

1 (*a*) R. Eisenberg and C. D. Meyer, *Acc. Chem. Res.*, 1975, **8**, 26; (*b*) M. H. Thiemens and W. C. Trogler, *Science*, 1991, **251**, 932; (*c*) *ACS Symp. Ser.*, 1995, **587**; (*d*) G. B. Ritcher-Addo and P. Legzdins, *Metal Nitrosyls*, Oxford University Press, New York, 1992.

2 E. R. S. Winter, *J. Catal.*, 1971, **22**, 158; F. Bottomley, *Acc. Chem. Res.*, 1978, **11**, 158; *Reactions of Coordinated Ligands*, ed. P. S. Braterman, Plenum, New York, 1989, vol. 2; *Methods in Nitric Oxide Research*, eds. M. Feelisch and J. S. Stamler, Wiley, Chichester, 1996.

3 D. E. Koshland, jun., *Science*, 1992, **258**, 1861; P. C. Ford, D. A. Wink and D. M. Stanbury, *FEBS Lett.*, 1993, **326**, 1; D. A. Wink and P. C. Ford, *Methods Enzymol.*, 1995, **7**, 14; A. R. Butler and D. L. H. Williams, *Chem. Soc. Rev.*, 1993, 233; D. R. Arnelle and J. S. Stamler, *Arch. Biochem. Biophys.*, 1995, **318**, 279; D. S. Bohle and C. H. Hung, *J. Am. Chem. Soc.*, 1995, **117**, 9584.

4 M. Fontecave and J. L. Pierre, *Bull. Soc. Chim. Fr.*, 1994, **131**, 620.

5 M. J. Clarke and J. B. Gaul, *Struct. Bonding* (*Berlin*), 1993, **81**, 144; P. J. Sadler, *Adv. Inorg. Chem.*, 1991, **36**, 1 and refs. therein; K. D. Karlin and Z. Tyeklar (Editors), *Bioinorganic Chemistry of Copper*, Chapman and Hall, New York, 1993; P. Legzdins, S. J. Rettig and S. F. Sayers, *J. Am. Chem. Soc.*, 1994, **116**, 12 105 and refs. therein; N. A. Davies, M. T. Wilson, E. Slade, S. P. Fricker, B. A. Murrer, N. A. Powell and G. R. Henderson, *Chem. Commun.*, 1997, 47.

6 M. J. Clarke, *J. Am. Chem. Soc.*, 1978, **100**, 5068.

7 E. A. M. F. Dahmen, *Electroanalysis: Theory and Application in Aqueous and Non Aqueous Media and Automated Chemical Control*, Elsevier, London, 1986.
8 S. E. Mazzetto, E. Tfouni and D. W. Franco, *Inorg. Chem.*, 1996, **35**, 3509.
9 S. Pell and J. N. Armor, *Inorg. Chem.*, 1973, **12**, 873.
10 S. S. Isied and H. Taube, *Inorg. Chem.*, 1974, **13**, 1545.
11 G. M. Brown, J. E. Sutton and H. Taube, *J. Am. Chem. Soc.*, 1978, **100**, 2767.
12 A. D. Becke, *Phys. Rev. A*, 1988, **38**, 3098.
13 C. Lee, W. Yang and R. G. Parr, *Phys. Rev. B*, 1988, **37**, 785.
14 GAUSSIAN 94, Revision B.2, M. J. Frisch, G. W. Trucks, H. B. Schlegel, P. M. W. Gill, B. G. Johnson, M. A. Robb, J. R. Cheesman, T. Keith, G. A. Petersson, J. A. Montgomery, K. Raghavachari, M. A. Al-Laham, V. G. Zakrzewski, J. V. Ortiz, J. B. Foresman, C. Y. Peng, P. Y. Ayala, W. Chen, M. W. Wong, J. L. Andres, E. S. Replogle, R. Gomperts, R. L. Martin, D. J. N. Fox, J. S. Binkley, D. J. Defrees, J. Baker, J. P. Stewart, M. Head-Gordon, O. C. Gonzalez and J. A. Pople, Gaussian, Inc., Pittsburgh, PA, 1995.
15 N. Godbout, D. R. Saluhub, J. Andzelm and E. Wimmer, *Can. J. Chem.*, 1992, **70**, 560.
16 HYPERCHEM 4, Hypercube, Inc., Toronto, CA, 1994.
17 J. H. Enemark and R. D. Feltham, *Coord. Chem. Rev.*, 1974, **13**, 339.
18 (*a*) J. N. Armor and M. Z. Hoffman, *Inorg. Chem.*, 1975, **14**, 444; (*b*) R. W. Callahan, G. M. Brown and T. J. Meyer, *J. Am. Chem. Soc.*, 1975, **97**, 894; (*c*) R. W. Callahan and T. J. Meyer, *Inorg. Chem.*, 1977, **16**, 574; (*d*) D. W. Pipes and T. J. Meyer, *Inorg. Chem.*, 1984, **23**, 2466; (*e*) I. A. Bagatin and H. E. Toma, *Spectrosc. Lett.*, 1996, **29**, 1409.
19 L. G. F. Lopes, E. E. Castellano, J. Z.-Schepctor, C. U. Davanzo, M. J. Clarke, A. Wieraszko and D. W. Franco, *Inorg. Chem.*, submitted.
20 R. Benedix and A. Vogler, *Inorg. Chim. Acta*, 1993, **204**, 189.
21 P. T. Manoharan and H. B. Gray, *J. Am. Chem. Soc.*, 1965, **87**, 3340.
22 A. F. Schreiner, P. J. Hauser, S. W. Lin, E. A. Hopcus, D. J. Hamm and J. D. Gunter, *Inorg. Chem.*, 1972, **11**, 880.
23 K. Nakamoto, *Infrared and Raman Spectra of Inorganic and Coordination Compounds*, 4th edn., Wiley, New York, 1986.
24 S. C. Silva, A. B. P. Lever and D. W. Franco, unpublished work.
25 J. W. Palmer and F. Basolo, *J. Inorg. Nucl. Chem.*, 1960, **15**, 279.
26 J. Mastone and J. N. Armor, *J. Inorg. Nucl. Chem.*, 1975, **37**, 473.
27 C. G. Kuehn and S. S. Isied, *Prog. Inorg. Chem.*, 1980, **27**, 153 and refs. therein.
28 G. J. Kubas and P. J. Vergamini, *Inorg. Chem.*, 1981, **20**, 2667.
29 R. C. Elder and M. Trkula, *Inorg. Chem.*, 1977, **16**, 1048.
30 C. A. Reed and W. R. Roper, *J. Chem. Soc., Dalton Trans.*, 1972, 1243.
31 F. Bottomley, *Acc. Chem. Res.*, 1978, **11**, 158.
32 A. Albert and P. E. Serjeant, *The Determination of Ionization Constants*, Chapman and Hall, Edinburgh, 1971.
33 J. B. Godwin and T. J. Meyer, *Inorg. Chem.*, 1971, **10**, 2150.
34 S. S. S. Borges, C. U. Davanzo, E. E. Castellano, J. Z.-Schepctor, S. C. Silva and D. W. Franco, *Inorg. Chem.*, submitted.
35 F. Bedioui, S. Trevin and J. Devynck, *J. Electroanal. Chem. Interfacial Electrochem.*, 1994, **377**, 295; V. Hampl, C. L. Walters and S. L. Archer, *Methods in Nitric Oxide Research*, eds. M. Feelisch and J. S. Stamler, Wiley, Chichester, 1996, ch. 21.
36 S. S. S. Borges, M. G. Gomes, L. C. G. Vasconcellos, H. A. S. Silva, R. M. Carlos, S. C. Silva and D. W. Franco, *Program and Abstracts of the Eighth Inter-American Photochemical Society Conference*, *Foz do Iguaçu*, 19–24th May, 1996, p. 81.
37 W. A. Cramer and D. B. Knaff, in *Energy Transduction in Biological Membranes: A textbook of Bioenergetics*, ed. Charles R. Cantor, Springer, New York, 1990, p. 334.
38 J. A. Rodriguez, A. Souza-Torsoni, D. W. Franco and M. Haun, *XXVI^a Reunião Anual da Sociedade Brasileira de Bioquímica e Biologia Molecular-SBBQ*, *Caxambú,* 3rd–6th May, 1997, S-32.

Received 13*th November* 1997; *Paper* 7/08164B